Laurentide Ice Sheet meltwater and abrupt climate change during the last glaciation

Heather W. Hill,[1] Benjamin P. Flower,[1] Terrence M. Quinn,[1]
David J. Hollander,[1] and Thomas P. Guilderson[2,3]

Received 21 June 2005; accepted 22 September 2005; published 18 February 2006.

[1] A leading hypothesis to explain abrupt climate change during the last glacial cycle calls on fluctuations in the margin of the North American Laurentide Ice Sheet (LIS), which may have routed fresh water between the Gulf of Mexico (GOM) and the North Atlantic, affecting North Atlantic Deep Water variability and regional climate. Paired measurements of $\delta^{18}O$ and Mg/Ca of foraminiferal calcite from GOM sediments reveal five episodes of LIS meltwater input from 28 to 45 thousand years ago (ka) that do not match the millennial-scale Dansgaard-Oeschger warmings recorded in Greenland ice. We suggest that summer melting of the LIS may occur during Antarctic warming and likely contributed to sea level variability during marine isotope stage 3.

Citation: Hill, H. W., B. P. Flower, T. M. Quinn, D. J. Hollander, and T. P. Guilderson (2006), Laurentide Ice Sheet meltwater and abrupt climate change during the last glaciation, *Paleoceanography*, *21*, PA1006, doi:10.1029/2005PA001186.

1. Introduction

[2] Abrupt climate changes during the last glaciation have been linked to variations in Atlantic thermohaline circulation. Numerical models demonstrate that an increased flux of fresh water to sites of deepwater formation decreases the strength of North Atlantic Deep Water (NADW), thereby reducing meridional heat transport and causing cooling/warming in the northern/southern high latitudes [*Ganopolski and Rahmstorf*, 2001; *Knutti et al.*, 2004]. This bipolar seesaw [*Broecker*, 1998] has been invoked to explain the antiphased relationship between climate changes in Antarctica and Greenland, where warmings in Antarctica precede those in Greenland by several thousand years [*Blunier and Brook*, 2001]. Additionally, the climate signature in Antarctica shows gradual temperature changes, while Greenland temperature is characterized by higher-frequency changes, including abrupt warmings that occur in decades, followed by slow coolings (Dansgaard-Oeschger (D/O) cycles).

[3] The North American Laurentide Ice Sheet (LIS) may have served as a source of fresh water to the North Atlantic during the last deglaciation, when ice sheet retreat led to the diversion of fresh water (meltwater and precipitation) from the Mississippi River drainage to the Hudson and St. Lawrence rivers [*Rooth*, 1982; *Broecker et al.*, 1988; 1989; *Shackleton*, 1989; *Flower and Kennett*, 1990; *Clark et al.*, 2001; *Flower et al.*, 2004]. Meltwater routing has been suggested as a potential control of high-frequency climate variability during intervals of intermediate ice volume, such as during marine isotope stage 3 (MIS 3) [*Clark et al.*, 2001]. However, evidence is needed to assess potential switches in freshwater routing during the millennial-scale D/O cycles, which are characterized by 5°–10°C oscillations in Greenland air temperature [*Dansgaard et al.*, 1993]. Here we test whether D/O warmings correspond to freshwater routing to the Gulf of Mexico (GOM) by reconstructing the $\delta^{18}O$ composition of seawater ($\delta^{18}O_{sw}$) using paired measurements of $\delta^{18}O_{calcite}$ ($\delta^{18}O_c$) and Mg/Ca of GOM foraminifera. Orca Basin (26°56.77′N, 91°20.74′W, Figure 1) in the northern GOM is ideally located to study freshwater input, including LIS meltwater, from the North American continent because of its proximal location to the mouth of the Mississippi River.

2. The $\delta^{18}O$ and Mg/Ca Analyses

[4] Core MD02-2551 was recovered from Orca Basin in July 2002 by the R/V *Marion Dufresne* as part of the International Marine Past Global Changes Study (IMAGES) program. The core was sampled at 2-cm intervals from 21 to 30 m. All samples were freeze dried prior to wet sieving, and then washed over a 63-μm mesh using deionized water. The ~60–70 planktonic foraminifera *G. ruber* (pink variety) were picked from the 250- to 355-μm-size fraction for isotopic and elemental analyses. The foraminifera were sonicated in methanol for 5 s to remove clays, and then weighed to assess down core dissolution effects. Mean *G. ruber* weights are similar throughout the interval and are comparable to surface-sediment samples [*LoDico et al.*, 2002]. The shells were gently crushed open between two glass plates and carefully homogenized using a razor blade. A ~50-μg aliquot was removed for stable isotopic analysis, which was performed at the College of Marine Science, University of South Florida, using a ThermoFinnigan Delta Plus XL dual-inlet mass spectrometer with an attached Kiel III carbonate

[1]College of Marine Science, University of South Florida, St. Petersburg, Florida, USA.
[2]Center for Accelerator Mass Spectrometry, Lawrence Livermore National Laboratory, University of California, Livermore, California, USA.
[3]Also at Department of Ocean Sciences and Institute of Marine Sciences, University of California, Santa Cruz, California, USA.

0883-8305/06/2005PA001186$12.00

Figure 1. Map of Orca Basin in the Gulf of Mexico showing location of core MD02-2551 (26°56.77′N, 91°20.74′W, 2248 m water depth) and the extent of the Laurentide Ice Sheet during marine isotope stage (MIS) 3 [from *Dyke et al.*, 2002].

preparation device. The isotopic data (Figure 2) are reported on the VPDB scale calibrated with NBS-19. Standard deviation for the $\delta^{18}O_c$ measurements is ±0.04‰, based on measurements of the standard NBS-19 analyzed with MD02-2551 foraminifer samples (n = 105).

[5] The remaining tests, weighing ~700 μg, were split into two aliquots that were cleaned separately for Mg/Ca analysis [*Barker et al.*, 2003]. This method involves an initial sonication to remove fine clays, oxidation of organic matter with a buffered peroxide solution, and a dilute acid leach that eliminates any adsorbed contaminants. Samples were dissolved in weak HNO_3 to yield calcium concentrations of ~20 ppm to minimize calcium concentration effects. The Mg/Ca ratios (Figure 2) were analyzed on a Perkin Elmer Optima 4300 dual-view inductively coupled plasma–optical emission spectrometer (ICP-OES). A standard instrument-drift correction technique was routinely used. The analytical precision for Mg/Ca determinations used in this study is <0.6% root-mean standard deviation (1σ), based on an ICP-MS calibrated standard solution. The pooled standard deviation of 70% replicate Mg/Ca analyses is ±2.5% (df = 318), which is equivalent to ~0.3°C. The $\delta^{18}O$ and Mg/Ca data can be accessed at the NOAA/NGDC World Data Center at http://www.ngdc.noaa.gov/paleo/paleo.html.

3. Age Model

[6] The age model developed for our record (Figure 2) is based on 18 AMS ^{14}C dates (Table 1) determined from monospecific samples (4–10 mg) of pink *G. ruber*, which were run at the Center for Accelerator Mass Spectrometry, Lawrence Livermore National Laboratory. The ^{14}C ages were corrected for a reservoir age of 400 years and converted to the GISP2 timescale (an approximation of calendar years) using a high-resolution radiocarbon calibration developed on sediment cores from the Cariaco Basin [*Hughen et al.*, 2004]. Inferred minimal changes in upwelling at the Orca Basin site indicate uncertainty in the reservoir correction is much better than 100 years. Age was also constrained by the Laschamp geomagnetic event [*Laj et al.*, 2000], which is recorded as a ~50 cm minimum in inclination at a depth of ~27.5 m (C. Kissel et al., personal communication, 2004). A peak in ^{10}Be, which coincides with the Laschamp event in sediment cores from the North Atlantic [*Robinson et al.*, 1995], straddles the

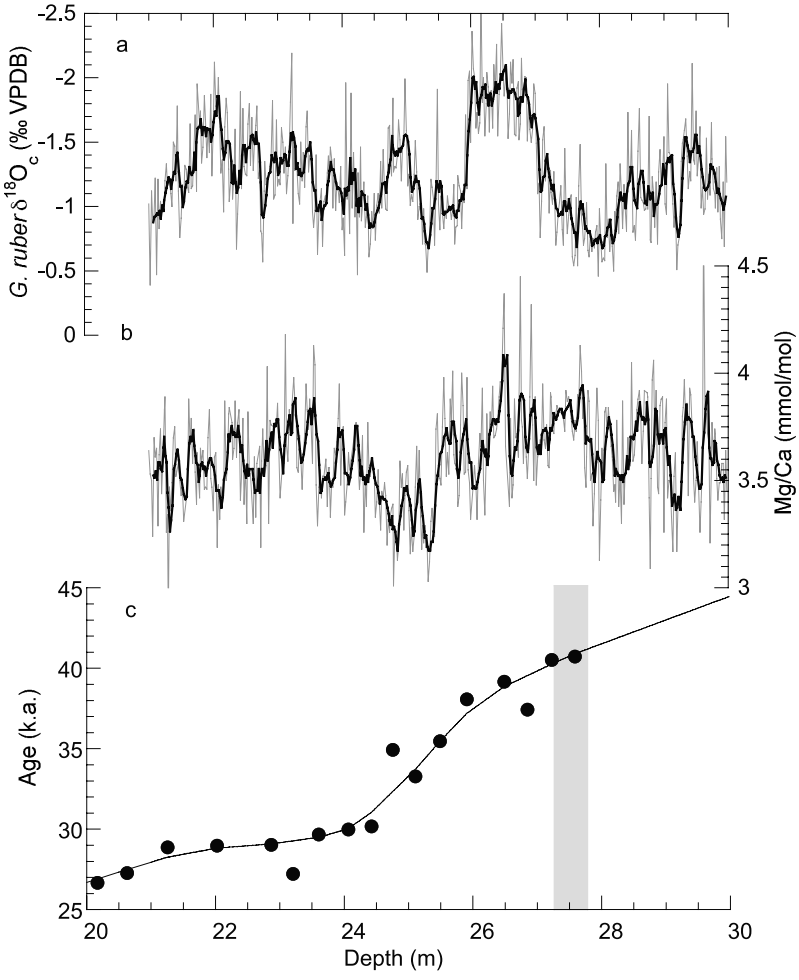

Figure 2. Raw $\delta^{18}O_c$ and Mg/Ca data and age model for MD02-2551: (a) $\delta^{18}O_c$ shown with five-point smooth fit, (b) Mg/Ca data shown with five-point smooth fit on *G. ruber* from Orca Basin core MD02-2551 versus depth in the core, and (c) age model for our interval based on 18 ^{14}C dates from *G. ruber*, which were converted to the Greenland Ice Sheet Project 2 (GISP2) timescale (an approximation of calendar years) using a Cariaco Basin radiocarbon calibration [*Hughen et al.*, 2004]. Age was constrained by the Laschamp geomagnetic event [*Laj et al.*, 2000], which is recorded as a sharp peak in inclination at a depth of ~27.5 m, as indicated by light grey bar (C. Kissel et al., personal communication, 2004).

$\delta^{18}O$ peak of interstadial 10 in the Greenland ice core record [*Yiou et al.*, 1997]. The Laschamp event was therefore assigned a calendar age of 40.9 ka based on the age of the δ ^{18}O peak of interstadial 10 on the Greenland GISP2 timescale [*Meese et al.*, 1997] (Figure 2).

[7] Depth in centimeters was converted to age by applying a weighted curve fit with a 40% smoothing factor and linearly extrapolating beyond the Laschamp event. This function fits a curve to the calibrated ^{14}C age control points, using the locally weighted least squares error method. Because of the uncertainty associated with radiocarbon dates of increasing age, including ^{14}C age plateaus at ~24 and ~28 ^{14}C ka [*Hughen et al.*, 2004], the weighted smooth fit provides a conservative estimate of depth versus age. Sedimentation rates range from 25 cm/kyr to 325 cm/kyr.

[8] Total error (1σ) on the age model ranges from 140 calendar years at ~26 ka to a maximum of 700 calendar years at ~40 ka. Error was determined by compounding the error on the ^{14}C measurements from this study (Table 1), the error on the ^{14}C measurements from the Cariaco record and the error from the GISP2/Cariaco calibration reported by *Hughen et al.* [2004]. Errors in ^{14}C were converted to calendar years using the Cariaco calibration. Calculating the error prior to 40 ka is difficult because of the uncertainty in the Cariaco calibration. Errors on the layer counting from the GISP2 record were not included in the total error analysis because we do not make conclusions about the absolute age of our events. Rather, we place our records on the GISP2 timescale to compare our results to Greenland air temperature history.

[9] We have also placed our data on the newly proposed age scale for the Greenland ice cores (SFCP 2004), which is based on ^{14}C dating of foraminifera in core MD95-2042, calibrated by paired ^{14}C and ^{230}Th measurements on corals

[*Shackleton et al.*, 2004] (see Auxiliary Material[1]). The conclusions that we report in the paper are the same regardless of which timescale we use for the Greenland ice core record.

4. Gulf of Mexico $\delta^{18}O$ of Seawater

[10] The *G. ruber* $\delta^{18}O_c$ values range from ~−0.5 to −2.5‰ (Figure 3). This 2‰ variability is not seen in the $\delta^{18}O_c$ of *N. dutertrei* (data not shown), an inferred deep dwelling planktonic foraminifer, suggesting that surface water phenomena are controlling the $\delta^{18}O_c$. The $\delta^{18}O_c$ record exhibits four oscillations about a mean value of −1.25‰, from 28 to 45 ka (Figure 3). The $\delta^{18}O_c$ values are more negative than the modern core top value of pink *G. ruber* (−1.7‰) during two of these oscillations (28.7–29.2 ka and 37.3–39.8 ka, Figure 3). Given that sea level was 63–93 m below present from 30 to 45 ka [*Siddall et al.*, 2003], which would result in an enrichment of the foraminifera $\delta^{18}O_c$ by ~0.5–0.75‰ based on the relationship 0.083‰ per 10 m sea level change [*Adkins and Schrag*, 2001], $\delta^{18}O_c$ values ≤−1.7‰ would indicate SSTs of 30°–32°C during MIS 3, which are unreasonably high compared to the modern average summer temperature in the GOM (29°C; June–September) [*Levitus*, 2004]. A change in $\delta^{18}O_{sw}$ associated with salinity variations is therefore required to explain the four negative oscillations recorded in the foraminiferal calcite.

[11] In order to isolate $\delta^{18}O_{sw}$, we subtract the temperature component from the $\delta^{18}O_c$ based on Mg/Ca data [*Flower et al.*, 2004]. The Mg/Ca ratio, a proxy for the temperature of foraminiferal calcification, is ideal for $\delta^{18}O_{sw}$ calculations because it is measured on an aliquot of the calcite sample used for $\delta^{18}O_c$. A *G. ruber* (pink) calibration, based on Atlantic sediment trap data [*Anand et al.*, 2003], was applied to the Mg/Ca measurements to calculate SST (Figure 3). We make the assumption that the effect of riverine input on the Mg/Ca values is minimal based on the large difference in Mg and Ca concentrations in the Mississippi River and the GOM (425 μM Mg versus 53 mM Mg; 870 μM Ca versus 10.3 mM Ca [*Briggs and Ficke*, 1978]). Despite the lower Mg/Ca ratio of Mississippi River water, oceanic Mg/Ca is not likely to be affected because the concentrations of Mg/Ca are low. A simple box model calculation shows that a 25% dilution of surface seawater (a likely maximum for *G. ruber* to withstand [*Hemleben et al.*, 1989]) would only decrease Mg/Ca values by <3%, which is within measurement error.

[12] The Mg-SST component was removed from the $\delta^{18}O_c$ using a temperature-$\delta^{18}O$ relationship [*Bemis et al.*, 1998] appropriate for *G. ruber* [*Thunnell et al.*, 1999], resulting in the $\delta^{18}O_{sw}$. The standard deviation for $\delta^{18}O_{sw}$ calculations is determined to be ±0.25‰, based on propagating the error through the analytical errors and the combined Mg-SST and SST-$\delta^{18}O$ relationships [*Beers*, 1957]. The variances used for the Mg-SST and SST-$\delta^{18}O$ equations are those reported in the literature. Variances for Mg/Ca and $\delta^{18}O$ were based on replicate analyses.

[1]Auxiliary material is available at ftp://ftp.agu.org/apend/pa/2005PA001186.

Table 1. Radiocarbon Ages for MD02-2551[a]

CAMS Number	Core Depth, m	^{14}C AMS Age, ka	±^{14}C Error	Calibrated Age, ka
108325	19.68	23.11	160	26.40
108326	20.16	23.46	70	26.70
108327	20.62	24.22	80	27.30
90835	21.25	25.41	130	28.90
108328	22.02	25.48	90	29.00
100591	22.86	25.54	130	29.05
100592	23.20	24.21	120	27.25
100593	23.60	26.28	140	29.70
100594	24.06	26.79	150	30.00
100595	24.42	27.30	160	30.20
90836	24.75	31.17	250	34.95
100596	25.10	29.59	210	33.30
100597	25.48	31.84	270	35.50
100598	25.90	33.67	340	38.10
108329	26.48	34.20	600	39.20
90837	26.84	33.28	320	37.45
100599	27.22	35.66	420	40.55
Laschamp event	27.50			40.90
100600	27.58	36.23	460	40.75
100601	28.06	35.38	410	40.30[b]
100665	28.46	34.80	500	40.00[b]
108330	29.20	37.83	300	41.30[b]
108331	29.88	33.17	180	37.30[b]

[a]CAMS is Center for Accelerator Mass Spectrometry, Lawrence Livermore National Laboratory; AMS is accelerator mass spectrometry.

[b]Samples not included in the age model because of stratigraphic inconsistencies. The ^{14}C ages at depths of 28.06, 28.46, and 29.88 m are younger than higher depths in the core. We choose not to use the ^{14}C age at 29.20 because it would require very large sedimentation rate changes from 30 cm/kyr to 200 cm/kyr. Although this is possible, we choose, instead, to linearly extrapolate beyond the Laschamp event, and we are conservative with interpretations in our data prior to 41 ka.

[13] The $\delta^{18}O_{sw}$ variations from core MD02-2551 have similarities to the global sea level record from MIS 3 [*Siddall et al.*, 2003] (Figure 3). However sea level fluctuations of <30 m during this interval [*Siddall et al.*, 2003] can explain only 0.25‰ of the >1‰ $\delta^{18}O_{sw}$ changes observed in our record, suggesting that changes in evaporation/precipitation (E-P) or freshwater input must be the dominant control on the $\delta^{18}O_{sw}$. We use the sea level record [*Siddall et al.*, 2003] to remove the contribution of global ice volume to the $\delta^{18}O_{sw}$, leaving the GOM $\delta^{18}O_{sw}$ residual ($\delta^{18}O_{GOM}$) (Figure 4). This was accomplished by converting sea level height to the $\delta^{18}O$ equivalent using the relationship 0.0083‰ per 1-m sea level change [*Adkins and Schrag*, 2001].

[14] The $\delta^{18}O_{GOM}$ values reflect changes in salinity, which result from a combination of source water variability and/or changes in the volume of water affecting the $\delta^{18}O_{GOM}$ signal. The $\delta^{18}O_{GOM}$ oscillates by up to 1.5‰, between more fresh versus more saline conditions, about a mean value of 0.45‰ (Figure 4). Major freshwater events, defined as intervals when the $\delta^{18}O_{GOM}$ reach values <0.45‰ and persist for >1.5 kyr, occurred from 31.7–34 ka and 37.2–39.8 ka (F2 and F4; Figure 4). The signatures of these two freshwater events are different, however: F2 is defined by a gradual change from more saline to more fresh conditions, while F4 is characterized by an abrupt freshening and an abrupt return to saline conditions. Three minor freshwater events, from 28.3–29.4,

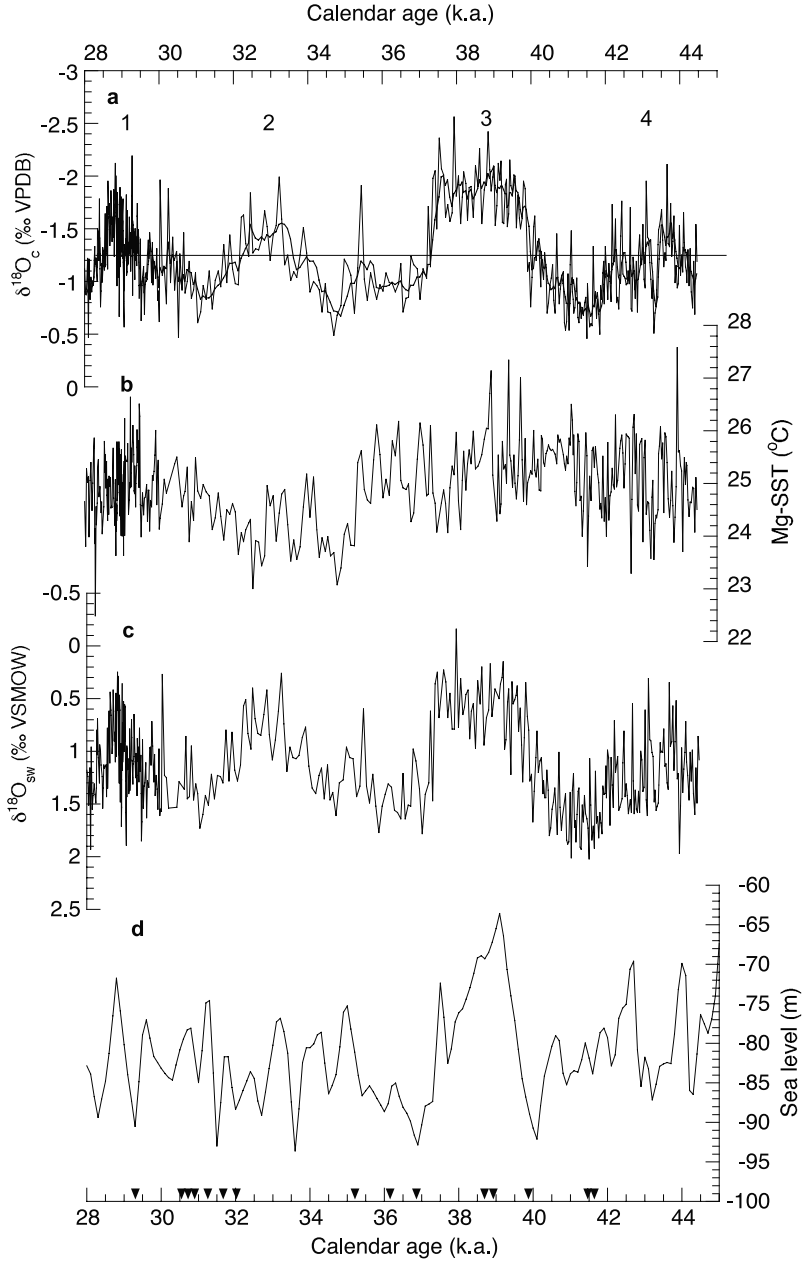

Figure 3. Paired $\delta^{18}O_c$ and Mg/Ca data on *G. ruber* from Orca Basin core MD02-2551 during MIS 3. (a) *G. ruber* $\delta^{18}O_c$, shown with five-point smooth fit. Mean value indicated by horizontal bar. Numbers refer to $\delta^{18}O_c$ oscillations referred to in text. (b) *G. ruber* Mg/Ca converted to SST using Mg/Ca = 0.38exp[0.09(SST (°C))] [*Anand et al.*, 2003]. (c) Calculated $\delta^{18}O_{sw}$ from $\delta^{18}O_c$ and Mg-SST using T(°C) = 14.9−4.8($\delta^{18}O_c - \delta^{18}O_{sw}$) [*Bemis et al.*, 1998]. The 0.27‰ was added to convert to Vienna SMOW. (d) Global sea level record [*Siddall et al.*, 2003]. Triangles on the bottom refer to intervals with ^{14}C dates.

35.0−35.5 and 42.9−43.8, also record values <0.45‰, but persist for <1.5 kyr (F1, F3 and F5; Figure 4).

5. Conversion to Sea Surface Salinity

[15] Conversion of $\delta^{18}O_{GOM}$ estimates to sea surface salinity (SSS) allows us to assess potential sources and magnitudes of freshwater flux to the GOM. SSS can be estimated using a $\delta^{18}O_{GOM}$ versus salinity relationship created for the GOM during MIS 3 (Figure 5). This relationship assumes conservative mixing between two end-members: high-salinity GOM waters ($\delta^{18}O_{sw}$ = 1.2‰ and S = 36.5 psu) and a low-salinity end-member. The low-salinity end-member is modeled using three different compositions: (1) a −3.5‰ value for GOM precipitation [*Bowen and Revenaugh*, 2003], and a Laurentide Ice Sheet (LIS) value ranging from (2) −15‰, reflecting the $\delta^{18}O$ of source waters that drained from the LIS [*Yapp and Epstein*,

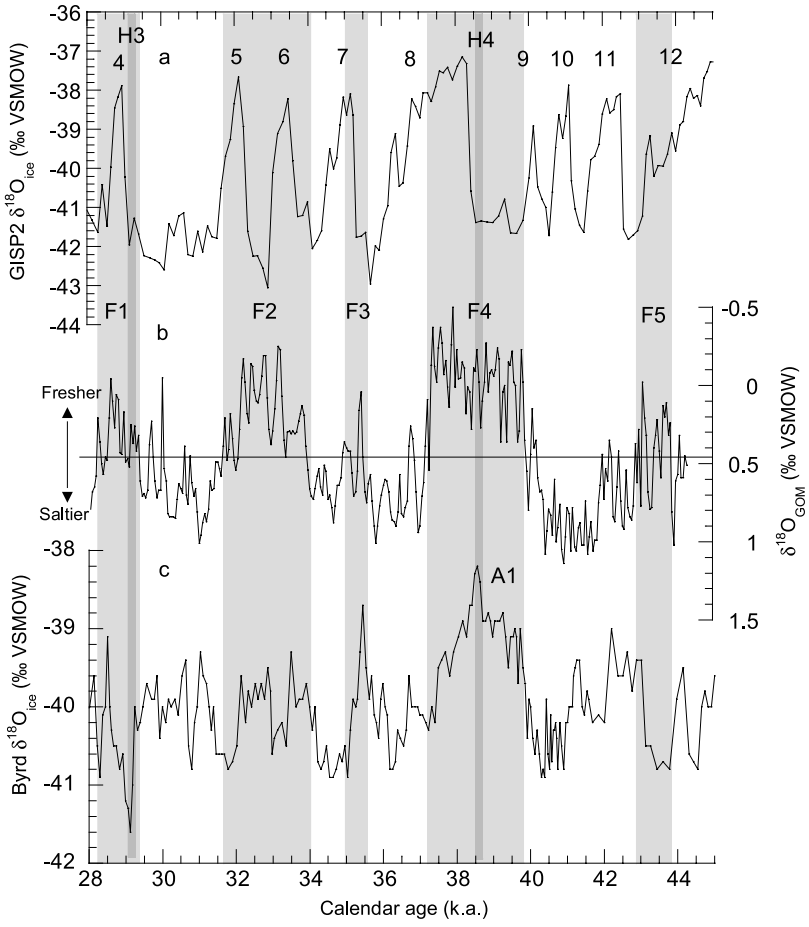

Figure 4. Comparison of Orca Basin $\delta^{18}O_{GOM}$ during MIS 3 with ice core records. (a) GISP2 $\delta^{18}O_{ice}$ [*Grootes et al.*, 1993]. (b) Orca Basin $\delta^{18}O_{GOM}$, with mean value indicated by horizontal bar. The $\delta^{18}O_{GOM}$ was calculated by subtracting global ice volume from the $\delta^{18}O_{sw}$ record. (c) Byrd $\delta^{18}O_{ice}$ record [*Johnsen et al.*, 1972] on the GISP2 timescale, based on synchronization of methane concentrations within the two ice cores [*Blunier and Brook*, 2001]. Numbers refer to Greenland interstadials. Light grey bars and the letter F (numbered 1–5) indicate freshwater events referred to in the text. Dark grey bars and letter H indicate Heinrich events. A1 refers to Antarctic warming event number 1 [*Blunier and Brook*, 2001].

1977], to (3) −30‰, the average composition of the LIS [*Dansgaard and Tauber*, 1969]. It should be noted that the more negative the zero salinity intercept, the smaller the changes in the estimated salinity variations (Figure 5). For example, a 1‰ change in $\delta^{18}O_{GOM}$ is equivalent to ∼1 psu on the −30‰ LIS mixing line, ∼2 psu on the −15‰ LIS mixing line and ∼8 psu on the −3.5‰ MR mixing line.

[16] Use of the −3.5‰ end-member would require changes in salinity of up to 10 psu (Figure 6) and a volume of water 3–5 times the largest historical flood [*Barry*, 1997], or >50X the annual precipitation in the GOM [*Ropelewski and Halpert*, 1996], lasting for 3 kyr during the largest event. It is possible that the isotopic composition of continental precipitation draining into the Mississippi River was more negative during MIS 3, because of changes in the altitude and/or sources of precipitation. However, a minimal change in the $\delta^{18}O$ composition of precipitation during MIS 3 is inferred from model simulations, which show similar $\delta^{18}O$ precipitation values between the Last Glacial Maximum and present [*Charles et al.*, 2001]. In addition, midcontinent speleothems, which reflect the changing isotopic composition of meteoric waters, record <0.5‰ variations in $\delta^{18}O$ during this interval [*Dorale et al.*, 1998]. We cannot rule out the possibility that increased precipitation over the GOM may reflect an intensification of the North American monsoon system, which is known to bring moisture to the region. However, the amount necessary to create the observed changes in the $\delta^{18}O_{GOM}$ record does not support oceanic precipitation as a primary control on this signal. In contrast, meltwater derived from the LIS with a $\delta^{18}O$ composition of −15 to −30‰ would require only modest changes in salinity: A −15‰ end-member for the LIS results in a salinity change of up to 3.5 psu, while a −30‰ end-member results in a change in salinity of up to 2 psu (Figure 6). Additionally, the average SSS using a −30‰ end-member is 35.5 ± 1 psu, which is within the modern salinity range in the GOM.

[17] We recognize that the source of fresh water likely changed through time and may have been a mixture of various sources (i.e., meltwater and precipitation), and

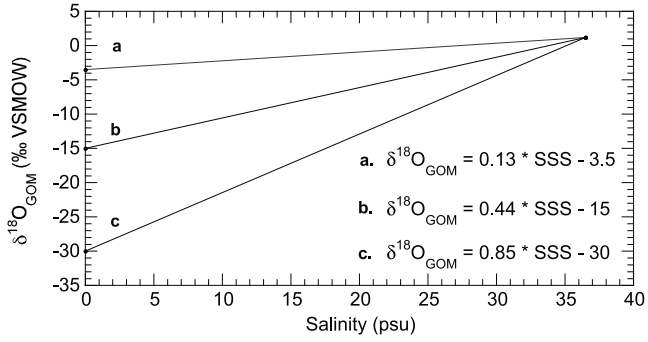

Figure 5. Mixing model for the Gulf of Mexico (GOM) during MIS 3. The $\delta^{18}O_{GOM}$ versus salinity relationship assumes conservative mixing between two end-members: high-salinity GOM waters ($\delta^{18}O_{sw}$ = 1.2‰ and S = 36.5 psu) and a low-salinity end-member. The low-salinity end-member is modeled using three different compositions: −3.5‰ (curve a) for GOM precipitation [*Bowen and Revenaugh*, 2003], −15‰ (curve b), reflecting the $\delta^{18}O$ of source waters that drained from the Laurentide Ice Sheet (LIS) [*Yapp and Epstein*, 1977], and −30‰ (curve c), the average composition of the LIS [*Dansgaard and Tauber*, 1969].

therefore the SSS calculations only reflect the end-member scenarios. Regardless, the most conservative estimate for salinity changes indicates a substantial meltwater contribution to $\delta^{18}O_{sw}$ in the GOM, particularly when the $\delta^{18}O$ composition of GOM waters were most depleted This explanation is supported by recent reconstructions of the LIS during MIS 3, which place the margin of the ice sheet within the MR drainage basin [*Dyke et al.*, 2002].

6. LIS Routing Hypothesis

[18] The uncertainty in the calibration of ^{14}C to calendar years precludes firm phase comparisons, but there appears to be no consistent relationship between $\delta^{18}O_{GOM}$ freshwater input and Greenland interstadials. The LIS routing hypothesis would predict that the nine D/O warmings (IS 4–12) that span 28–45 ka [*Grootes et al.*, 1993] should correspond to freshwater routing to the GOM [*Clark et al.*, 2001], but only five $\delta^{18}O_{GOM}$ freshwater events are recorded in the Orca Basin during this interval (Figure 4). There is no age model that we can construct with the ^{14}C dates that would allow the $\delta^{18}O_{GOM}$ record from Orca Basin to be on the same timing as the D/O cycles in Greenland. In addition, the Laschamp event coincides with a warming in Greenland (IS 10), but a positive $\delta^{18}O$ excursion (more saline) in our record. If each of the D/O warmings corresponds to freshwater routing to the GOM, we would expect to see a negative $\delta^{18}O_{GOM}$ excursion in our record during this interval. Although freshwater routed to eastern outlets may have led to NADW reductions and coolings in Greenland, the timing and number of $\delta^{18}O_{GOM}$ freshwater events to the GOM suggest that a simple routing hypothesis cannot explain all of the MIS 3 Greenland interstadials. It appears that the D/O warmings cannot be attributed to changes in the strength of NADW associated with southward routing of meltwater by the LIS, which may

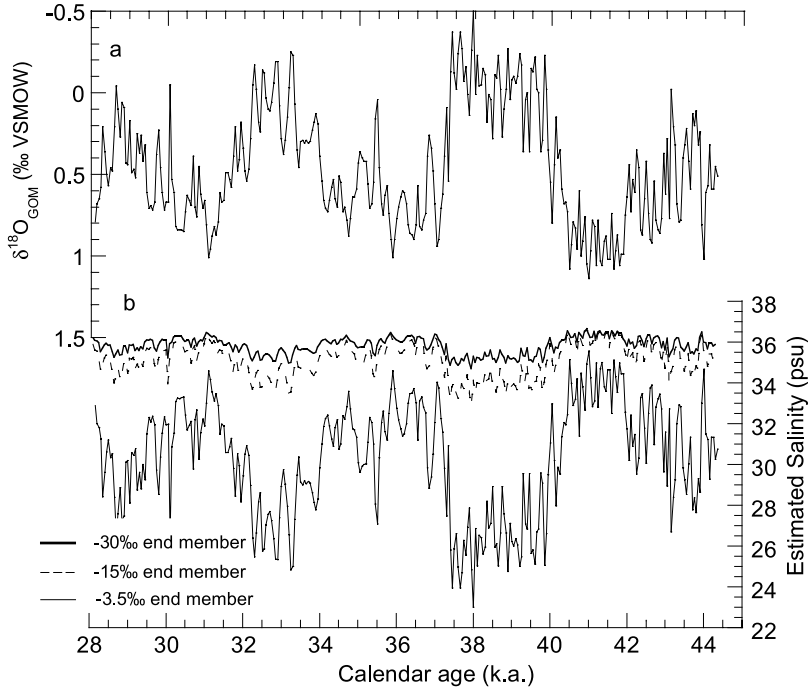

Figure 6. GOM sea surface salinity (SSS) reconstructions from 28 to 45 ka. SSS is based on the conversion of $\delta^{18}O_{GOM}$ to salinity using a mixing model with three freshwater end-members (see Figure 5): (a) $\delta^{18}O_{GOM}$ and (b) estimated salinity. The most conservative estimate for salinity changes indicates a substantial meltwater contribution to $\delta^{18}O_{sw}$ in the GOM.

help explain why it has been difficult to find NADW changes during each of the D/O cycles [*Curry et al.*, 1999; *Hagen and Keigwin*, 2002; *Vautravers et al.*, 2004]. Additionally, SST in the GOM does not appear to be coupled to Greenland air temperature.

[19] The $\delta^{18}O_{GOM}$ record has similarities to the Antarctic air temperature record [*Johnsen et al.*, 1972], the global sea level record from MIS 3 [*Siddall et al.*, 2003], and to the classic MIS 3 benthic $\delta^{18}O$ record off Portugal [*Shackleton et al.*, 2000]. Freshwater events in the GOM have a tendency to coincide with intervals of Antarctic warming. In particular, the largest freshwater event (F4) occurred at the same time as the largest warming in Antarctica (A1 centered at 39 ka; Figure 4) and a 30-m rise in sea level also at 39 ka [*Siddall et al.*, 2003].

[20] Our $\delta^{18}O_{GOM}$ record suggests summer melting on the southern margin of the LIS during Antarctic warming, as also observed during the last deglaciation [*Flower et al.*, 2004]. This provides evidence to support a recent modeling study that suggests that the Northern Hemisphere ice sheets contributed one half of the global sea level rises observed between 35 and 65 ka [*Rohling et al.*, 2004]. Our results are also consistent with a new coupled atmosphere-ocean simulation that predicts that freshwater discharge into the Gulf of Mexico would contribute to Antarctic warming [*Knutti et al.*, 2004]. LIS melting associated with the A1 warming in Antarctica may have provided a positive feedback for Southern Hemisphere warming through changes in the strength of NADW. Similarly, our results indicate that growth/decay cycles of the LIS may have been decoupled from Greenland air temperature history during MIS 3. Our finding underscores recent work suggesting that the LIS (which is influenced by summer melting) does not follow Greenland air temperature (which is influenced by winter temperatures, particularly during stadials) and that seasonality is an important aspect of abrupt climate change [*Denton et al.*, 2005].

[21] **Acknowledgments.** We thank the IMAGES program, Yvon Balut, and Laurent Labeyrie for a productive cruise on the R/V *Marion Dufresne* in 2002. This work was supported in part by the National Science Foundation under grant OCE-0318361 to B.P.F. and T.M.Q. We thank the IMAGES program also for collection of the core. Ethan Goddard provided technical assistance with data collection. We also thank Luis Garcia-Rubio and Gary Mitchum for assistance with error analysis, Richard Poore and Kelly Kilbourne for comments on the manuscript, and Jyotika Virmani and the USF Paleo lab members for useful discussions. The manuscript was improved through the suggestions of several anonymous reviewers and Larry Peterson, who served as Editor. Radiocarbon analyses were performed under the auspices of the U.S. Department of Energy by the University of California Lawrence Livermore National Laboratory (contract W-7405-Eng-48).

References

Adkins, J. R., and D. P. Schrag (2001), Pore fluid constraints on deep ocean temperature and salinity during the last glacial maximum, *Geophys. Res. Lett.*, *28*, 771–774.

Anand, P., H. Elderfield, and M. H. Conte (2003), Calibration of Mg/Ca thermometry in planktonic foraminifera from a sediment trap time series, *Paleoceanography*, *18*(2), 1050, doi:10.1029/2002PA000846.

Barker, S., M. Greaves, and H. Elderfield (2003), A study of cleaning procedures used for foraminiferal Mg/Ca paleothermometry, *Geochem. Geophys. Geosyst.*, *4*(9), 8407, doi:10.1029/2003GC000559.

Barry, J. M. (1997), *Rising Tide—The Great Mississippi Flood of 1927 and How it Changed America*, 524 pp., Simon and Schuster, New York.

Beers, Y. (1957), *Introduction to the Theory of Error*, 66 pp., Addison-Wesley, Boston, Mass.

Bemis, B. E., J. H. Spero, J. Bijma, and D. W. Lea (1998), Reevaluation of the oxygen isotopic composition of planktonic foraminifera: Experimental results and revised paleotemperature equations, *Paleoceanography*, *13*(2), 150–160.

Blunier, T., and E. J. Brook (2001), Timing of millennial-scale climate change in Antarctica and Greenland during the last glacial period, *Science*, *291*, 109–112.

Bowen, G. J., and J. Revenaugh (2003), Interpolating the isotopic composition of modern meteoric precipitation, *Water Resour. Res.*, *39*(10), 1299, doi:10.1029/2003WR002086.

Briggs, J. C., and J. F. Ficke (1978), Quality of rivers of the United States, 1975 water year, *U.S. Geol. Surv. Open File Rep.*, *78–200*, 436 pp.

Broecker, W. S. (1998), Paleocean circulation during the last deglaciation: A bipolar seesaw?, *Paleoceanography*, *13*(2), 119–121.

Broecker, W. S., M. Andree, W. Wolfli, H. Oeschger, G. Bonani, J. Kennett, and D. Peteet (1988), The chronology of the last deglaciation: Implications to the cause of the Younger Dryas event, *Paleoceanography*, *3*(1), 1–19.

Broecker, W. S., J. P. Kennett, B. P. Flower, J. T. Teller, S. Trumbore, G. Bonani, and W. Wolfli (1989), Routing of meltwater from the Laurentide Ice Sheet during the Younger Dryas cold episode, *Nature*, *341*, 318–321.

Charles, C. S., D. Rind, R. Healy, and R. Webb (2001), Tropical cooling and the isotopic composition of precipitation in general circulation model simulations of the ice age climate, *Clim. Dyn.*, *17*(7), 489–502.

Clark, P. U., S. J. Marshall, G. K. C. Clarke, S. W. Hostetler, J. M. Licciardi, and J. T. Teller (2001), Freshwater forcing of abrupt climate change during the last glaciation, *Science*, *293*, 283–287.

Curry, W. B., T. M. Marchitto, J. F. McManus, D. W. Oppo, and K. L. Laarkamp (1999), Millennial-scale changes in ventilation of the thermocline, intermediate, and deep water of the glacial North Atlantic, in *Mechanisms of Global Climate Change at Millennial Time Scales*, *Geophys. Monogr. Ser.*, vol. 112, edited by P. U. Clark, R. S. Webb, and L. D. Keigwin, pp. 59–76, AGU, Washington, D. C.

Dansgaard, W., and H. Tauber (1969), Glacier oxygen-18 content and Pleistocene ocean temperatures, *Science*, *166*, 499–502.

Dansgaard, W., et al. (1993), Evidence for general instability of past climate from a 250-kyr ice-core record, *Nature*, *364*, 218–220.

Denton, G. H., R. B. Alley, G. C. Comer, and W. S. Broecker (2005), The role of seasonality in abrupt climate change, *Quat. Sci. Rev.*, *24*, 1159–1182.

Dorale, J. A., R. L. Edwards, E. Ito, and L. A. Gonzalez (1998), Climate and vegetation history of the mid-continent from 75 to 25 ka: A speleothem record from Crevice Cave, Missouri, USA, *Science*, *282*, 1871–1874.

Dyke, A. S., J. T. Andrews, P. U. Clark, J. H. England, G. H. Miller, J. Shaw, and J. J. Veillette (2002), The Laurentide and Innuitian ice sheets during the Last Glacial Maximum, *Quat. Sci. Rev.*, *21*, 9–31.

Flower, B. P., and J. P. Kennett (1990), The Younger Dryas cool episode in the Gulf of Mexico, *Paleoceanography*, *5*(6), 949–961.

Flower, B. P., D. W. Hastings, H. W. Hill, and T. M. Quinn (2004), Phasing of deglacial warming and Laurentide Ice Sheet meltwater in the Gulf of Mexico, *Geology*, *32*, 597–600.

Ganopolski, A., and S. Rahmstorf (2001), Rapid changes of glacial climate simulated in a coupled climate model, *Nature*, *409*, 153–158.

Grootes, P. M., M. Stuiver, J. W. C. White, S. Johnsen, and J. Jouzel (1993), Comparison of oxygen-isotope records from the GISP2 and GRIP Greenland ice cores, *Nature*, *366*, 552–554.

Hagen, S., and L. D. Keigwin (2002), Sea-surface temperature variability and deep water reorganization in the subtropical North Atlantic during isotope stage 2–4, *Mar. Geol.*, *189*, 145–162.

Hemleben, C., M. Spindler, and O. R. Anderson (1989), *Modern Planktonic Foraminifera*, 363 pp., Springer, New York.

Hughen, K., S. Lehman, J. Southon, J. Overpeck, O. Marchal, C. Herring, and J. Turnbull (2004), ^{14}C Activity and global carbon cycle changes over the past 50,000 years, *Science*, *303*, 202–207.

Johnsen, S. J., H. B. Clausen, W. Dansgaard, and C. C. Langway (1972), Oxygen isotope profiles through Antarctic and Greenland ice sheets, *Nature*, *235*, 429–434.

Knutti, R., J. Fluckiger, T. F. Stocker, and A. Timmermann (2004), Strong hemispheric coupling of glacial climate through freshwater discharge and ocean circulation, *Nature*, *430*, 851–856.

Laj, C., C. Kissel, A. Mazaud, J. E. T. Channell, and J. Beer (2000), North Atlantic paleointensity stack since 75 ka (NAPIS-75) and the duration of the Laschamp event, *Philos. Trans. R. Soc. London, Ser. A*, *358*, 1009–1025.

Levitus, S. (2004), National Oceanographic Data Center World Ocean Atlas 1994, http://www.cdc.noaa.gov/cdc/data.nodc.woa94.html, Earth Syst. Res., Phys. Sci. Div., Natl. Oceanic and Atmos. Admin., Boulder, Colo.

LoDico, J. M., D. W. Hastings, B. P. Flower, and T. M. Quinn (2002), A multi-proxy approach to distinguish between changes in SST and meltwater input in the Gulf of Mexico back to MIS 3, *Eos Trans. AGU*, *83*(47), Fall Meet. Suppl., Abstract PP62A-0331.

Meese, D. A., A. J. Gow, R. B. Alley, G. A. Zielinski, P. M. Grootes, M. Ram, K. C. Taylor, P. A. Mayewski, and J. F. Bolzan (1997), The Greenland Ice Sheet Project 2 depth-age scale: Methods and results, *J. Geophys. Res.*, *102*, 26,411–26,423.

Robinson, C., G. M. Raisbeck, F. Yiou, B. Lehman, and C. Laj (1995), The relationship between ^{10}Be and geomagnetic field strength records in central North Atlantic sediments during the last 80 ka, *Earth Planet. Sci. Lett.*, *136*, 551–557.

Rohling, E. J., R. Marsh, N. C. Wells, M. Siddall, and N. R. Edwards (2004), Similar meltwater contributions to glacial sea level changes from Antarctic and northern ice sheets, *Nature*, *430*, 1016–1021.

Rooth, C. G. H. (1982), Hydrology and ocean circulation, *Prog. Oceanogr.*, *11*, 131–149.

Ropelewski, C. F., and M. S. Halpert (1996), Quantifying Southern Oscillation-precipitation relationships, *J. Clim.*, *9*, 1043–1059.

Shackleton, N. J. (1989), Deep trouble for climate change, *Nature*, *342*, 616–617.

Shackleton, N. J., M. A. Hall, and E. Vincent (2000), Phase relationships between millennial-scale events 64,000–24,000 years ago, *Paleoceanography*, *15*(6), 565–569.

Shackleton, N. J., R. G. Fairbanks, T. Chiu, and F. Parrenin (2004), Absolute calibration of the Greenland time scale: Implications for Antarctic time scales and for $\Delta^{14}C$, *Quat. Sci. Rev.*, *23*, 1513–1522.

Siddall, M., E. J. Rohling, A. Almogi-Labin, C. Hemleben, D. Meischner, I. Schmelzer, and D. A. Smeed (2003), Sea-level fluctuations during the last glacial cycle, *Nature*, *423*, 853–858.

Thunnell, R., E. Tappa, C. Pride, and E. Kincaid (1999), Sea-surface temperature anomalies associated with the 1997–1998 El Niño recorded in the oxygen isotope composition of planktonic foraminifera, *Geology*, *27*, 843–846.

Vautravers, M. J., N. J. Shackleton, C. Lopez-Martinez, and J. O. Grimalt (2004), Gulf Stream variability during marine isotope stage 3, *Paleoceanography*, *19*, PA2011, doi:10.1029/2003PA000966.

Yapp, C. J., and S. Epstein (1977), Climatic implications of D/H ratios of meteoric water over North America (9,500–22,000 B.P.) as inferred from ancient wood cellulose C-H hydrology, *Earth Planet. Sci. Lett.*, *34*, 333–350.

Yiou, F. G., et al. (1997), Beryllium 10 in the Greenland Ice Core Project ice core at Summit, Greenland, *J. Geophys. Res.*, *102*, 26,783–26,794.

B. P. Flower, H. W. Hill, D. J. Hollander, and T. M. Quinn, College of Marine Science, University of South Florida, 140 7th Avenue South, St. Petersburg, FL 33701-5016, USA. (bflower@marine.usf.edu; hhill@marine.usf.edu)

T. P. Guilderson, Center for Accelerator Mass Spectrometry, Lawrence Livermore National Laboratory, University of California, Livermore, CA 94550, USA.